Homotopy analysis of the Lippmann–Schwinger equation for seismic wavefield modelling in strongly scattering media

Morten Jakobsen,[1] Xingguo Huang[1] and Ru-Shan Wu[2]

[1]*Department of Earth Science, University of Bergen, Allegaten* 41, 5020 *Bergen, Norway. E-mail:* Morten.Jakobsen@uib.no
[2]*Institute of Earth and Planetary Physics, University of California, Santa Cruz, CA* 95060, *USA*

SUMMARY
We present an application of the homotopy analysis method for solving the integral equations of the Lippmann–Schwinger type, which occurs frequently in acoustic and seismic scattering theory. In this method, a series solution is created which is guaranteed to converge independent of the scattering potential. This series solution differs from the conventional Born series because it contains two auxiliary parameters ϵ and h and an operator H that can be selected freely in order to control the convergence properties of the scattering series. The ϵ-parameter which controls the degree of dissipation in the reference medium (that makes the wavefield updates localized in space) is known from the so-called convergent Born series theory; but its use in conjunction with the homotopy analysis method represents a novel feature of this work. By using $H = I$ (where I is the identity operator) and varying the convergence control parameters h and ϵ, we obtain a family of scattering series which reduces to the conventional Born series when $h = -1$ and $\epsilon = 0$. By using $H = \gamma$ where γ is a particular pre-conditioner and varying the convergence control parameters h and ϵ, we obtain another family of scattering series which reduces to the so-called convergent Born series when $h = -1$ and $\epsilon \geq \epsilon_c$ where ϵ_c is a critical dissipation parameter depending on the largest value of the scattering potential. This means that we have developed a kind of unified scattering series theory that includes the conventional and convergent Born series as special cases. By performing a series of 12 numerical experiments with a strongly scattering medium, we illustrate the effects of varying the (ϵ, h, H)-parameters on the convergence properties of the new homotopy scattering series. By using $(\epsilon, h, H) = (0.5, -0.8, I)$ we obtain a new scattering series that converges significantly faster than the convergent Born series. The use of a non-zero dissipation parameter ϵ seems to improve on the convergence properties of any scattering series, but one can now relax on the requirement $\epsilon \geq \epsilon_c$ from the convergent Born series theory, provided that a suitable value of the convergence control parameter h and operator H is used.

Key words: Numerical approximations and analysis; Multiple scattering theory; Waveform modelling; Homotopy analysis.

1 INTRODUCTION

There exist a range of different numerical methods for seismic wavefield modelling (Carcione *et al.* 2002), including differential equation methods (e.g., Robertsson *et al.* 2012) and integral equation methods (Pike & Sabatier 2000; Jakobsen 2012; Oristaglio & Blok 2012; Jakobsen & Wu 2016; Malovichko *et al.* 2018). The majority of researchers in the seismic community use differential equation methods (Carcione *et al.* 2002), but the integral equation approach has actually several advantages compared with the differential equation approach: (1) it is naturally target oriented (Haffinger *et al.* 2013; Huang *et al.* 2019), (2) it gives the sensitivity matrix directly in terms of Green's functions (Jakobsen & Ursin 2015)

which is convenient for uncertainty estimation (Eikrem *et al.* 2019) and (3) it is compatible with the use of domain decomposition and renormalization methods from modern physics (Jakobsen & Wu 2016, 2018).However, the integral equation approach can be less efficient than the differential equation approach, depending on how it is implemented (Jakobsen & Wu 2018; Malovichko *et al.* 2018; Jakobsen *et al.* 2019). An integral equation solution based on matrix inversion can be very accurate, but very memory-depending and costly (Jakobsen & Wu 2018). Efficient implementations of the integral equations approach are typically based on the use of iterative methods and /or scattering series solutions (Jakobsen & Wu 2016, Malovichko *et al.* 2018; Huang *et al.* 2019a,b; Jakobsen *et al.* 2019).

Many geophysicists are familiar with the scattering series of Born that one can easily obtain from the Lippmann–Schwinger equation via simple iteration (Jakobsen & Wu 2016). However, the Born series represents an example of a so-called naive perturbation expansion which is only guaranteed to converge in the special case of relatively small contrasts (Kirkinis 2008; Jakobsen & Wu 2016). To obtain a convergent scattering scattering series in the presence of strong contrasts, it may be required to use a non-perturbative method for strongly nonlinear systems. Previously, researchers have developed convergent scattering series solutions of the Lippmann–Schwinger equation by using renormalization procedures (Wu *et al.* 2007; Abubakar & Habashy 2013; Jakobsen *et al.* 2016, 2019; Osnabrugge *et al.* 2016). In this study, however, we have employed the so-called homotopy analysis method (HAM), which is based on concepts and ideas form topology (Liao 2003; Hetmaniok *et al.* 2014).

The HAM used in this study was developed by Liao (1998, 2003, 2004, 2009, 2012, 2014). However, the development of related globally convergent homotopy methods for solving nonlinear equations started around 1976 (see Watson 1989). Historically, there have been several attempts to apply homotopy methods to model and invert geophysical data (see Watson 1989), but the paper of Huang & Greenhalgh (2019) appears to represent the first geophysical application of the modern hHAM developed by Liao (2003), which differs from the one discussed by Watson (1989). In any case, the homotopy methods allows one to solve operator equations of any kind by using ideas and concepts of topology, which is a branch of pure and applied mathematics dealing with quantities that are preserved during continuous deformations. A homotopy describes a continuous transformation between two states and has been compared with the concept of scale-invariance in renormalization group theory (Palit & Datta 2016; Jakobsen *et al.* 2019a; Pfeffer 2019). The HAM have been used to solve a range of different nonlinear problems, ranging from heat conduction problems (Abbasbandy 2006) to problems within theoretical physics (Pfeffer 2019). Most applications of the HAM is based on a differential operator formulation, but there have also been successful attempts to solve integral equations of the Fredholm and Volterra types using the HAM (see Hetmaniok *et al.* 2014).

Although the HAM may potentially be very useful for practical nonlinear inversion of seismic waveform data (see Han *et al.* 2005; Fu & Han 2006), we shall focus on the forward problem. This is partially because there is still an important need for more work on the nonlinear direct scattering problem (Jakobsen *et al.* 2019a,b) and the corresponding nonlinear inverse scattering problem is much more difficult to solve due to its ill-posed nature. It will be demonstrated that the HAM can be used to construct a scattering series solution of the Lippmann–Schwinger equation in the context of seismic wavefield modelling. Although such convergent scattering series have been developed on the basis of renormalization methods in the past (Abubakar & Habashy 2013; Osnabrugge *et al.* 2016; Jakobsen *et al.* 2019a), we think it is interesting to study convergence properties of the direct scattering series solution from different perspectives, since this may give us new ideas and insights that may be useful for future studies of nonlinear inverse scattering as well as direct scattering problems.

In Section 2, we present fundamental equations and establish our notation. In Section 3, we present a general method for obtaining convergent series solutions of nonlinear operator equations that does not depend on any parameter being small. In Section 4, we derive a convergent scattering series solution of the Lippmann–Schwinger equation. In Section 5, we show that the conventional

Born series and the renormalized Born series of Osnabrugge *et al.* (2016) and Huang *et al.* (2019) represent a special case of the HAM series. In Section 6, we demonstrate that the HAM series converges for strongly scattering media where the conventional Born series diverges. In Section 7, we also provide some ideas for further work.

2 THE LIPPMANN–SCHWINGER EQUATION AND CONVENTIONAL BORN SERIES

The scalar wave equation in the frequency domain (the inhomogeneous Helmholtz equation) can be written as (Morse & Feshbach 1953; Osnabrugge *et al.* 2016; Huang *et al.* 2019a,b)

$$\left(\nabla^2 + k^2(\mathbf{x})\right)\psi(\mathbf{x}) = -S(\mathbf{x}),\tag{1}$$

where $k(\mathbf{x})$ is the wavenumber at position $\mathbf{x}$. Following Osnabrugge *et al.* (2016), we now decompose the actual medium with wavenumber $k(\mathbf{x})$ into an arbitrary homogeneous dissipative reference medium with complex wavenumber k_d given by $k_d^2 = k_0^2 + i\epsilon$ (where ϵ is an arbitrary small positive number) and a corresponding complex scattering potential $V(\mathbf{x})$ (with compensating gain, rather than dissipation). It follows that

$$\left(\nabla^2 + k_d^2\right)\psi(\mathbf{x}) = -S(\mathbf{x}) - V(\mathbf{x})\psi(\mathbf{x}),\tag{2}$$

where

$$V(\mathbf{x}) = k^2(\mathbf{x}) - k_d^2.\tag{3}$$

The second term on the right-hand side of eq. (2) represents the so-called equivalent sources. By treating the contrast sources just like real sources, one can derive the Lippmann–Schwinger equation (Jakobsen & Ursin 2015):

$$\psi(\mathbf{x}) = \psi^{(0)}(\mathbf{x}) + \int_\Omega d\mathbf{x}'\, G^{(0)}(\mathbf{x} - \mathbf{x}') V(\mathbf{x}')\psi(\mathbf{x}'),\tag{4}$$

where $G^{(0)}(\mathbf{x} - \mathbf{x}')$ is Green's function for the homogeneous reference medium, which satisfies

$$\left(\nabla^2 + k_d^2\right) G^{(0)}(\mathbf{x} - \mathbf{x}') = -\delta(\mathbf{x} - \mathbf{x}').\tag{5}$$

Note that the introduction of a non-zero imaginary part ϵ to the squared wavenumber k_0^2 in the homogeneous reference medium makes the energy associated with Green's function finite and the wave fields more localized (Osnabrugge *et al.* 2016; Huang *et al.* 2019b; Jakobsen *et al.* 2019a). Although most workers tend to set ϵ to zero, the use of a non-zero ϵ parameter improves the convergence properties of any scattering series (Abubakar & Habashy 2013; Osnabrugge *et al.* 2016; Huang *et al.* 2019b; Jakobsen *et al.* 2019a).

In symbolic operator notation, the Lippmann–Schwinger equation (4) can be written as

$$\psi = \psi^{(0)} + G^{(0)} V \psi,\tag{6}$$

where the scattering potential operator V is local (but see Jakobsen & Wu 2017) and can be represented by a diagonal matrix in the real-space representation (Jakobsen & Ursin 2015). The above equation has the following exact formal solution:

$$\psi = (I - G^{(0)} V)^{-1} \psi^{(0)}\tag{7}$$

where I is the identity operator.

Solution (7) is valid independently of the contrast volume, but it involves the inversion of a huge operator or matrix (in the coordinate representation), which can be very costly in the case of a realistic model. In principle, one could try to solve the Lippmann–Schwinger equation by iteration. The well-known Born series can be

regarded as the simplest possible iterative solution of the Lippmann–Schwinger equation and can be presented as

$$\psi = \sum_{m=0}^{\infty} \psi_m \tag{8}$$

where $\psi_0 = \psi^{(0)}$ and

$$\psi_m = G^{(0)} V \psi_{m-1}, \quad m = 1, 2, 3, \dots . \tag{9}$$

The Born series is very popular due to its simplicity. However, the Born series represents an example of a naive perturbation expansion (Kirkinis 2008) which is only guaranteed to converge if the contrast is relatively small, in the sense that the largest eigenvalue of the operator $G^{(0)}V$ must be smaller than unity (Weinberg 1963; Newton 2002; Osnabrugge *et al.* 2016).

3 THE HOMOTOPY ANALYSIS METHOD

The HAM can be used to solve operator equations of the form (Liao 2003)

$$N[\psi] = 0, \tag{10}$$

where N denotes a nonlinear operator and ψ is the unknown function (or state vector). The first step is to define the homotopy operator $\mathcal{H}$ by (Liao 2003)

$$\mathcal{H}[\Phi, \lambda] \equiv (1 - \lambda)L[\Phi(\lambda) - \psi_0] - \lambda h H N[\Phi(\lambda)], \tag{11}$$

where $\lambda \in [0, 1]$ is the so-called embedding parameter, $h \neq 0$ is the so-called convergence control parameter, H is a convergence control operator (see Section 4), ψ_0 is our initial guess of the solution to eq. (10) and L is an auxiliary linear operator that can be selected arbitrarily as long as $L[0] = 0$.

By setting $\mathcal{H}[\Phi, \lambda] = 0$ we get the so-called zero-order deformation equation (Liao 2003)

$$(1 - \lambda)L[\Phi(\lambda) - \psi_0] = \lambda h H N[\Phi(\lambda)]. \tag{12}$$

If $\lambda = 0$ then $L[\Phi(0) - \psi_0] = 0$, which implies that $\Phi(0) = \psi_0$. If $\lambda = 1$ then $N[\Phi(1)] = 0$, which implies that $\Phi(1) = \psi$, where ψ is the solution of eq. (10) we are looking for. A gradual change in the embedding parameter λ from 0 to 1 therefore means a continuous transition of $\Phi(\lambda)$ from the initial guess ψ_0 to the exact solution ψ of the original eq. (10).

If we now expand the auxiliary field $\Phi(\lambda)$ into a Maclaurin series with respect to the embedding parameter λ then we obtain (Liao 2003)

$$\Phi(\lambda) = \Phi(0) + \sum_{m=1}^{\infty} \frac{1}{m!} \frac{\partial^m \Phi(\lambda)}{\partial \lambda^m}\Big|_{\lambda=0} \lambda^m. \tag{13}$$

By introducing the definition (Liao 2003)

$$\psi_m \equiv \frac{1}{m!} \frac{\partial^m \Phi(\lambda)}{\partial \lambda^m}\Big|_{\lambda=0}, \quad m = 1, 2, 3, \dots, \tag{14}$$

the above eq. (13) can be expressed as (Liao 2003)

$$\Phi(\lambda) = \Phi(0) + \sum_{m=1}^{\infty} \psi_m \lambda^m. \tag{15}$$

If the above series (15) is convergent for $\lambda = 1$ then the solution we are looking for is given by (Liao 2003)

$$\psi = \sum_{m=0}^{\infty} \psi_m. \tag{16}$$

It is of course not obvious that the series (15) is convergent for $\lambda = 1$, but by adjusting the auxiliary parameter h and the auxiliary operator H we can make sure that this series is indeed convergent (Liao 2003).

In order to determine the different ψ_m terms, we now differentiate the left and right side of the zeroth-order deformation eq. (12) m times with respect to the auxiliary parameter λ, divide the result by $m!$ and set $\lambda = 0$. In this way suggested by Liao (2003), we obtain the so-called mth-order deformation equation ($m > 0$):

$$L[\psi_m - \chi_m \psi_{m-1}] = hHR_m, \tag{17}$$

where

$$\chi_m = \begin{cases} 0 \text{ if } m \leq 1 \\ 1 \text{ if } m \geq 2 \end{cases} \tag{18}$$

and

$$R_m = \frac{1}{(m-1)!} \left(\frac{\partial^{m-1}}{\partial \lambda^{m-1}} N\left[\sum_{i=0}^{\infty} \psi_i \lambda^i \right] \right)_{\lambda=0}. \tag{19}$$

The different R_m parameters will depend on the nature of the nonlinear operator N. In the next section, we shall evaluate the R_m parameters for the nonlinear operator corresponding with the Lippmann–Schwinger equation.

The selection of the convergence control parameter h is very important. In order to select a suitable value of h, one can either use the h-parameter curve method or an optimization method (Liao 2003; Hetmaniok *et al.* 2014). We shall discuss the selection of h in connection with the results we have obtained for the homotopy analysis of the Lippmann–Schwinger equation.

4 HOMOTOPY ANALYSIS OF THE LIPPMANN–SCHWINGER EQUATION

Hetmaniok *et al.* (2014) discuss the usage of the HAM for solving nonlinear and linear integral equations of the second kind. However, their analysis is restricted to 1-D media and slightly different from the analysis presented below. In order to derive a convergent scattering series solution of the Lippmann–Schwinger equation based on the HAM, we define the linear and nonlinear integral operators L and N by

$$L[\psi] = \psi, \quad N[\psi] = \psi - \psi^{(0)} - G^{(0)} V \psi, \tag{20}$$

By using the above definitions of the linear and nonlinear operators L and N in conjunction with the mth-order deformation equation (17), we obtain

$$\psi_m = \chi_m \psi_{m-1} + hHR_m. \tag{21}$$

By using the definition of the nonlinear operator N given in eq. (20) in conjunction with the expression for the R_m parameters in eq. (18), we get

$$R_m = \frac{1}{(m-1)!} \frac{\partial^{m-1}}{\partial \lambda^{m-1}} \left[\sum_{i=0}^{\infty} \psi_i \lambda^i - \psi^{(0)} - G^{(0)} V \sum_{i=0}^{\infty} \psi_i \lambda^i \right]_{\lambda=0}. \tag{22}$$

The above equation implies that

$$R_m = \frac{1}{(m-1)!} \Big((m-1)! \psi_{m-1} - (1 - \chi_m) \psi^{(0)} \\ - (1 - m)! G^{(0)} V \psi_{m-1} \Big), \tag{23}$$

or

$$R_m = \psi_{m-1} - \frac{(1-\chi_m)}{(1-m)!}\psi^{(0)} - G^{(0)}V\psi_{m-1}. \tag{24}$$

By using the above expression for R_m in conjunction with the recursive formula (21), we obtain

$$\psi_1 = hH\left(\psi_0 - \psi^{(0)} - G^{(0)}V\psi_0\right), \tag{25}$$

and for $m \geq 2$:

$$\psi_m = \mathcal{M}\psi_{m-1}, \tag{26}$$

where

$$\mathcal{M} \equiv I + hH - hHG^{(0)}V. \tag{27}$$

Eqs (25) and (A1) for the first- and higher-order terms in the homotopy analysis scattering series represent the main results of this paper. This HAM iterative solution of the Lippmann–Schwinger equation differs from the conventional Born series via the convergence control parameter h and the operator H that can be selected arbitrarily to ensure that the series is convergent. The HAM series converges if the spectral radius σ of M is smaller than unity; which can occur even if the spectral radius of the operator G_0V is larger than unity; that is, when the conventional scattering series of Born diverges.

5 COMPARISON WITH EXISTING ANALYTICAL RESULTS

If we use our freedom to set $\psi_0 = \psi(0)$, $h = -1$ and $H = I$ then the homotopy series in eqs (25) and (26) reduces to the conventional Born series (9). As discussed earlier, the conventional Born series have a rather small range of convergence, since the largest eigenvalue of the operator $G^{(0)}V$ must be smaller than unity.

Osnabrugge *et al.* (2016) presented a modified Born series (CBS) which is guaranteed to converge independent of the scattering potential. If we set $\psi_0 = \gamma\psi^{(0)}$ where $\gamma = iV/\epsilon$ is the pre-conditionner of Osnabrugge *et al.* (2016) then it follows from eq. (23) that

$$\psi_1 = hH\left(I - \gamma^{-1} - G^{(0)}V\right)\psi_0. \tag{28}$$

If we now set $h = -1$ and $H = \gamma$ then the above equation becomes

$$\psi_1 = M\psi_0, \tag{29}$$

where

$$M \equiv I - \gamma + \gamma G^{(0)}V. \tag{30}$$

Also, it follows from equation that

$$\psi_m = M\psi_{m-1}, \tag{31}$$

which implies that the convergent Born series of Osnabrugge *et al.* (2016) is a special case of our new HAM series.

A comparison of eqs (26) & (27) and (30) & (31) clearly suggests that we have generalized the convergent Born series of Osnabrugge *et al.* (2016). We can construct a family of convergent Born series similar to the convergent Born series of Osnabrugge *et al.* (2016) if we set $H = \gamma$ but use different values of the convergence control parameter h. The CBS is based on the use of a dissipative reference medium, which makes Green's function finite and localized (Osnabrugge *et al.* 2016; Huang *et al.* 2019b; Jakobsen *et al.* 2019a). Since our generalized convergent Born series based on HAM contains the additional convergence control parameter h, we can decrease the value of the dissipation parameter ϵ if we compensate

by using a suitable h-value. The convergence control parameter h is a global convergence parameter, in the sense that it acts globally on the whole model, whereas the dissipation parameter ϵ can be regarded as a local convergence parameter, since a higher value for ϵ implies a higher degree of wavefield localization. By a suitable choice of the local and global convergence control parameters ϵ and h we can accelerate the convergence of the HAM series. This point will be illustrated in the next section dealing with numerical experiments based on a strongly scattering seismic model. By introducing an imaginary part to the wavevector of the background medium, we make the total energy represented by the background Green's function finite and localized. The imaginary term in the background medium is compensated exactly by an imaginary term in the scattering potential. Therefore, the final solution remains the same as the solution without any dissipation.

6 NUMERICAL RESULTS AND DISCUSSION

We performed a series of 12 different numerical experiments to study the effects of the auxiliary parameters (ϵ, h, H) on the convergence properties of the HAM for solving the Lippmann–Schwinger equation. The numerical experiments are based on a resampled version of the SEG/EAGE salt model (Fig. 1, left). We used a homogeneous reference medium with wave speed $c_0 = 2870$ m s^{-1} (Fig. 1, right). We employed a single delta function source with frequency 10 Hz located in the middle of the top of the model and we used a grid size equal to 5 m in each direction. In each experiment, we used one of the combinations of the (ϵ, h, H) parameters given in Table 1 and generated a scattering series solution of the Lippmann–Schwinger equation by using the recursive formulae (25)–(27).

We quantified the convergence properties of the different scattering series by calculating the normalized overall error δ_k as a function of the number of iterations k, where

$$\delta_k = ||\sum_{i=1}^{k}\psi_i - \psi^{(r)})||/||\psi^{(r)}||, \tag{32}$$

and $\psi^{(r)}$ is a reference solution obtained by solving eq. (7) via matrix inversion (see Fig. 2), which is exact apart from very small numerical discretization errors (Jakobsen 2012). In each numerical experiment, we iterated until the normalized overall error became smaller than 10^{-3} (in the case of convergence) or larger than 10 (in the case of divergence). However, this stopping criterion is of course flexible and dependent on the desired accuracy.

If the scattering series diverges then the resulting wavefield (Fig. 3) will of course look very different from the reference wavefield (Fig. 2). If the scattering series converges in the sense that the overall normalized error becomes smaller than 10^{-3} than the resulting wavefield (Fig. 4) will necessarily be very similar to the true wavefield (Fig. 2). Since the resulting wavefield is independent of the auxiliary parameters in the case of convergence, we focus on the behaviour of δ_k rather than the wavefield itself.

In numerical experiments 1–6 (Fig. 5), we assumed $H = I$ and varied the dissipation parameter ϵ and the convergence control parameter h. As discussed in the previous section, when $\epsilon = 0$ and $h = -1$, the numerical results correspond with the conventional Born series, whereas the use of different ϵ- and h-values represents different modifications of the conventional Born series. Clearly, one can see from the blue curve in Fig. 5 that the conventional Born series corresponding with $\epsilon = 0$ and $h = -1$ diverges for this strongly scattering medium. When $\epsilon = 0$ and $h = -0.95$ corresponding with
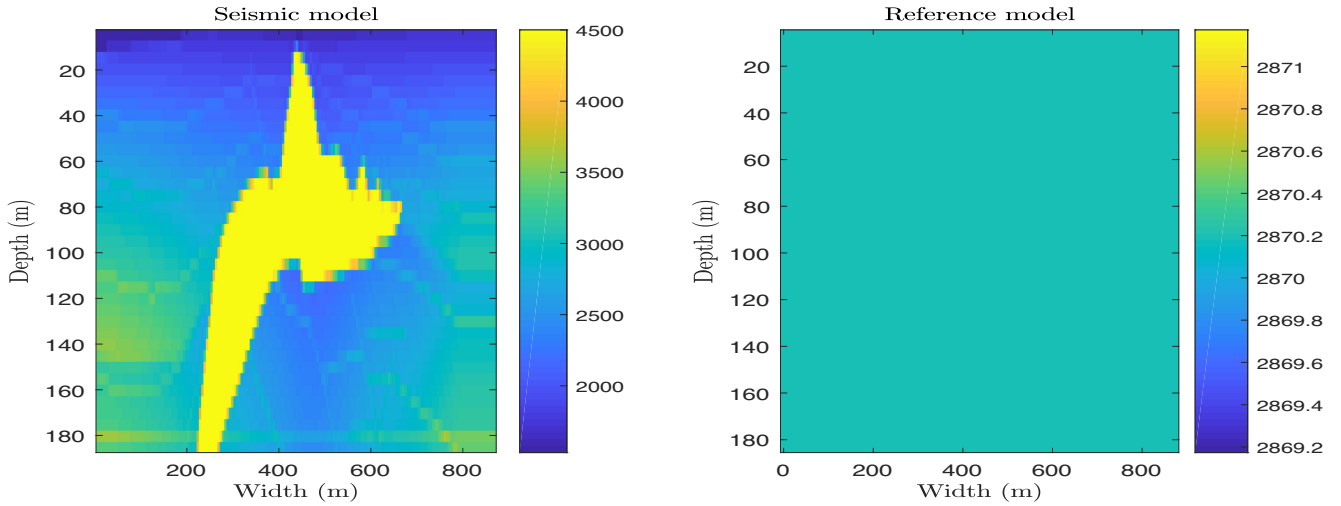
Figure 1. The true velocity model and the homogeneous reference model.

Table 1. Convergence control parameters used in four different numerical experiments focusing on the convergence properties of the homotopy analysis method. The parameter ϵ_c is the critical value which is required for the convergent Born series of Osnabrugge *et al.* (2016) to converge. The colour refers to the different colors used in Fig. 5 (experiments 1–6) and Fig. 6 (experiments 7–12).

Experiment	ϵ/ϵ_c	h	H	Colour	$\|M\|$	$\sigma(M)$
1	0.00	01.000	I	1.46	1.06	b
2	0.00	00.950	I	1.40	1.03	g
3	0.00	00.900	I	1.35	0.99	r
4	0.00	00.800	I	1.27	0.94	c
5	0.00	00.100	I	1.01	0.97	m
6	0.50	00.800	I	0.96	0.82	k
7	1.00	−1.000	γ	0.94	1.98	b
8	0.50	−1.000	γ	0.85	1.93	g
9	0.50	−0.500	γ	0-92	1.09	r
10	0.50	−0.250	γ	0.96	0.93	c
11	0.50	−0.125	γ	0.98	0.96	m
12	0.25	−0.125	γ	0.96	1.00	k

the green curve in Fig. 5, the scattering series still diverges. When $\epsilon = 0$ and $h = −0.9$ corresponding with the red curve in Fig. 5, the scattering series is starting to converge, but extremely slowly. When $\epsilon = 0$ and $h = −0.8$ corresponding with the cyan curve in Fig. 5, the scattering series converges faster. When $\epsilon = 0$ and $h = −0.1$ corresponding to the black curve in Fig. 5, the scattering series is still convergent, but the convergence rate is much smaller than when using $h = −0.8$. When $\epsilon = 0.5$ and $h = −0.8$ corresponding to the black curve in Fig. 5 than the scattering series converges faster than for all the other experiments 1-5. Therefore, it appears that the use of a non-zero ϵ-value in conjunction with an optimal h-value helps to accelerate an already convergent scattering series.

In numerical experiments 7–12 (Fig. 6), we assumed $H = \gamma$ and varied the dissipation parameter ϵ as well as the convergence control parameter h. When $\epsilon \leq \epsilon_c$ where ϵ_c is a critical value depending on the velocity model and $h = −1$ then the numerical results corresponds with the convergent Born series of Osnabrugge *et al.* (2016), whereas the use of different ϵ and h-parameters correspond with different modifications of the convergent Born series of Osnabrugge *et al.* (2016). Clearly, one can see from the blue curve in Fig. 6 that the convergent Born series of Osnabrugge *et al.* (2016) corresponding with $\epsilon = \epsilon_c$ and $h = −1$ is indeed convergent. When $h = −1$ but

$\epsilon = 0.5\epsilon_c$ corresponding to the green curve in Fig. 6, the scattering series is as expected divergent. When $\epsilon = 0.5\epsilon_c$ and $h = −0.5$ corresponding with the red curve in Fig. 6, the scattering series is still divergent. However, when $\epsilon = 0.5\epsilon_c$ and $h = −0.25$ corresponding with the cyan curve in Fig. 6, the scattering series become convergent again. When $\epsilon = 0.5\epsilon_c$ and $h = −0.125$ corresponding with the curve in Fig. 6, the scattering series is still convergent, but the convergence rate is smaller than when using $h = −0.25$. When using $\epsilon = 0.25\epsilon_c$ corresponding with the black curve in Fig. 6 the scattering series converges extremely slowly. Therefore, it appears that the ϵ and h-parameters corresponding with the original convergent Born series of Osnabrugge *et al.* (2016) are optimal when $H = \gamma$.

Fig. 7 represents a comparison of the optimal HAM series (the black curve in Fig. 6 corresponding to $\epsilon = 0.5$, $h = −0.8$ and $H = I$) and the original convergent Born series of Osnabrugge *et al.* (2016) (the blue curve in Fig. 6 corresponding with $\epsilon = 1$, $h = −1$ and $H = −\gamma$). Clearly, one can see that the optimal HAM series requires much less iterations than the original convergent Born series. Therefore, one can say that we have generalized and improved on the convergent Born series of Osnabrugge *et al.* (2016) by using the HAM.

The auxiliary parameters ϵ and h may be referred to as local and global convergence control parameters, respectively. This is because a non-zero ϵ value leads to dissipation in the reference medium (and gain in the scattering potential), which makes the wavefield update more localized in space; and different h-values are associated with different degrees of global wavefield scaling. Having both local and global convergence control parameters in addition to the auxiliary convergence control operator H makes this HAM very general and flexible.

7 CONCLUDING REMARKS

We have used the HAM to derive a general scattering series solution of the Lippmann–Schwinger equation which is guaranteed to converge independent of the scattering potential, provided that one select the dissipation parameter ϵ as well as the convergence control parameter h and operator H in a suitable manner. We have found that the conventional Born series and the convergent Born series of Osnabrugge *et al.* (2016) are special cases of the new scattering series based on HAM. We have performed a series of 12 numerical
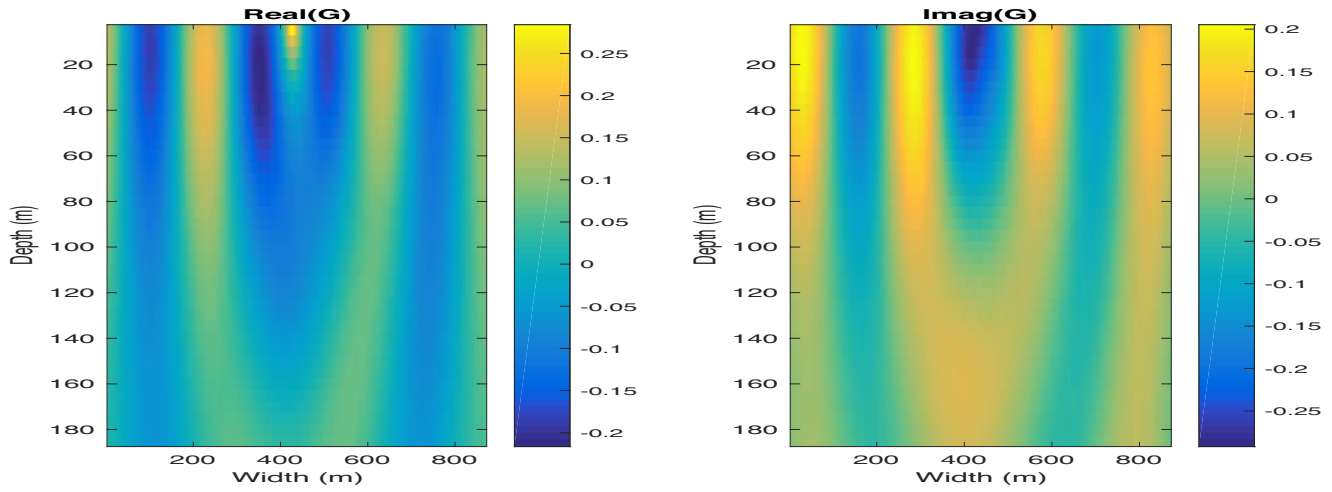
Figure 2. Real and imaginary parts of the frequency-domain wavefield at 10 Hz computed by solving the Lippmann–Schwinger equation exactly using a real space matrix representation.
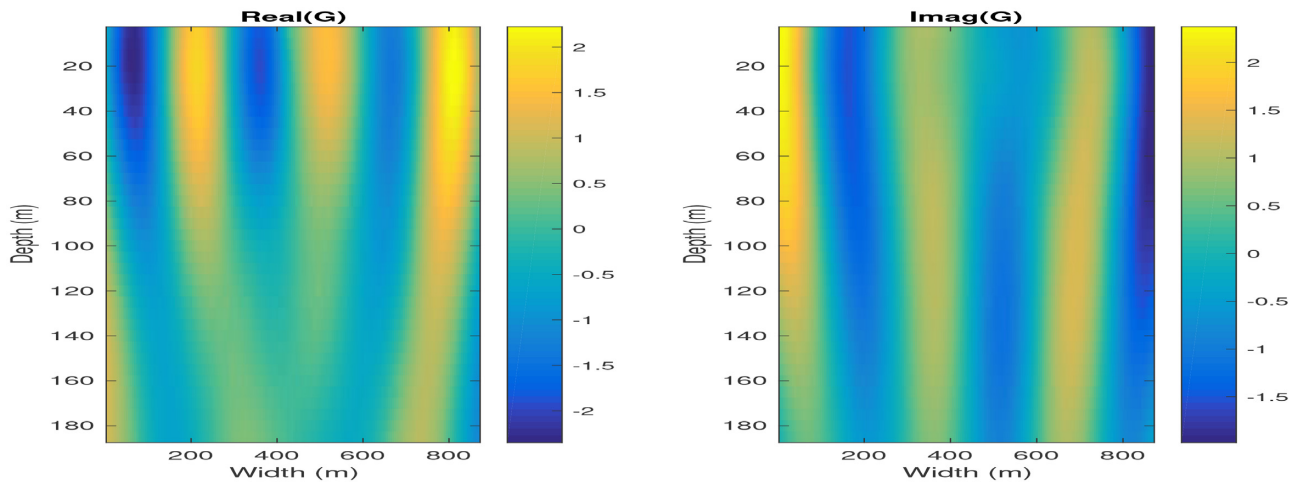
Figure 3. The real and imaginary parts of the frequency- domain wavefield at 10 Hz computed using the HAM series with auxiliary parameters corresponding to experiment 1 in Table 1.
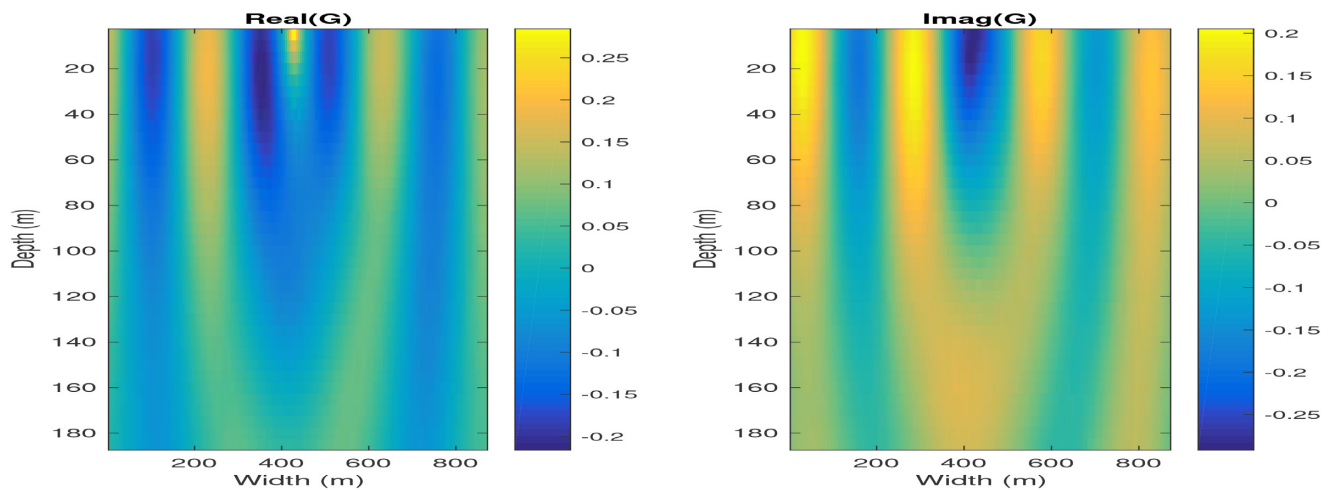
Figure 4. The real and imaginary parts of the frequency-domain wavefield at 10 Hz computed using the HAM series with auxiliary parameters corresponding with experiment 2 in Table 1.
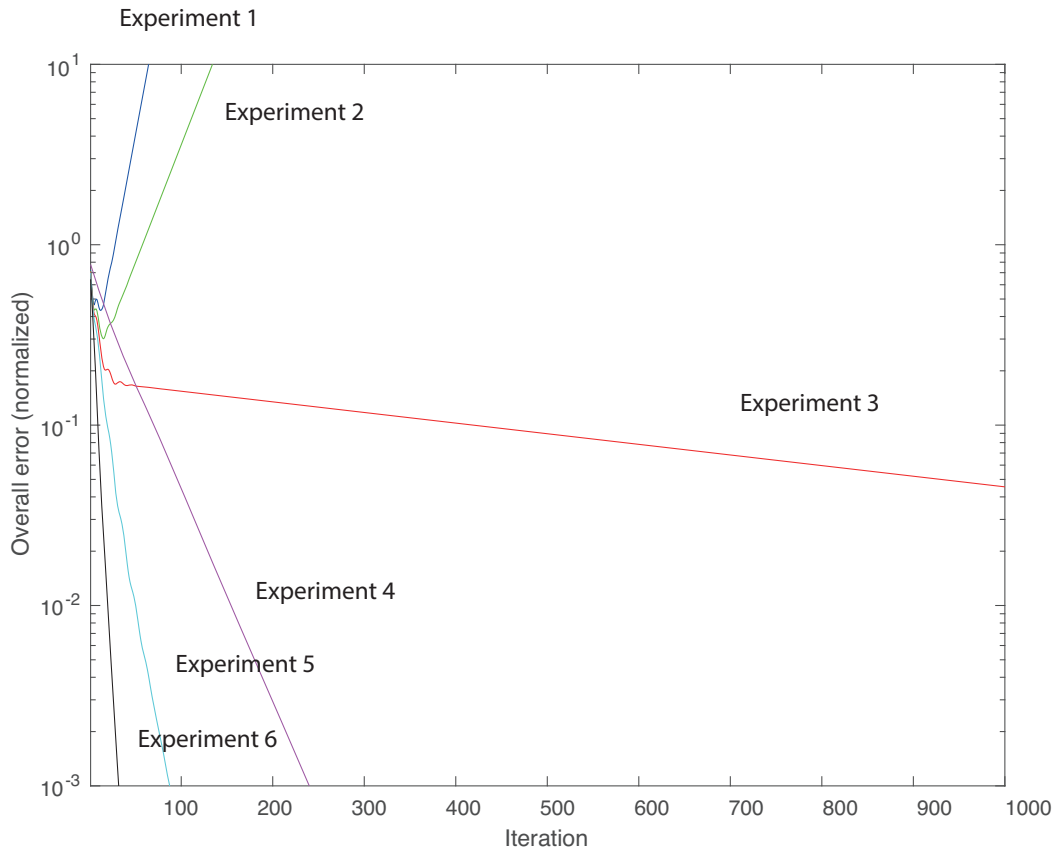
Figure 5. Comparison of overall errors versus the number of iterations for numerical experiments 1–6 described in Table 1.
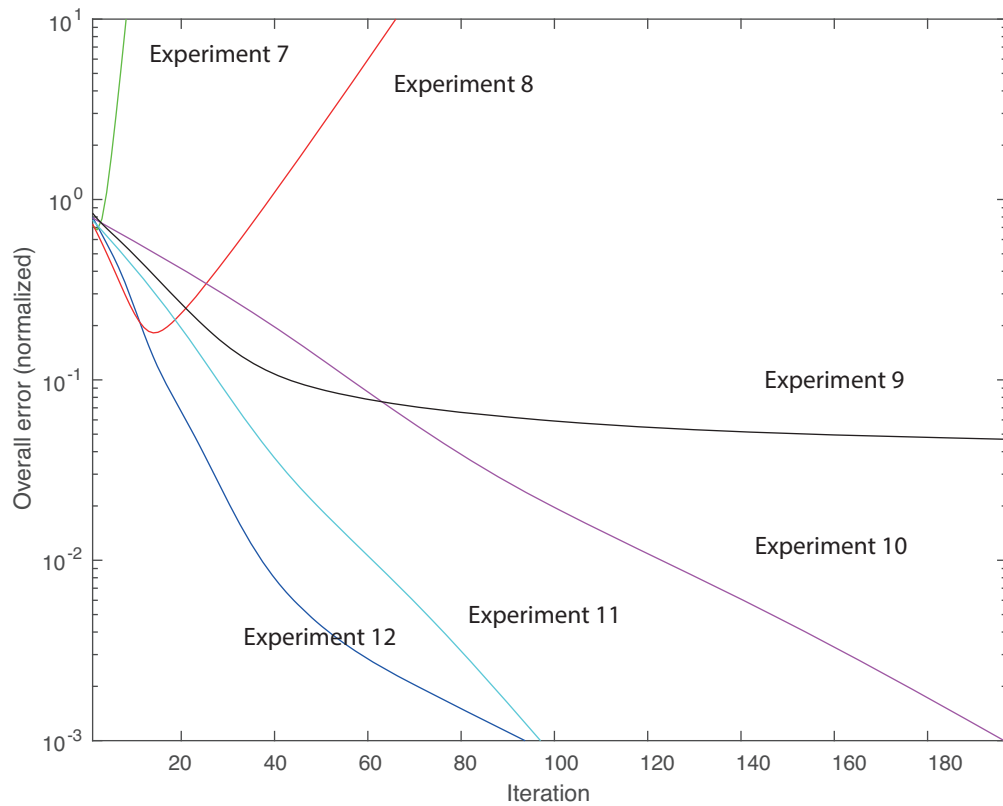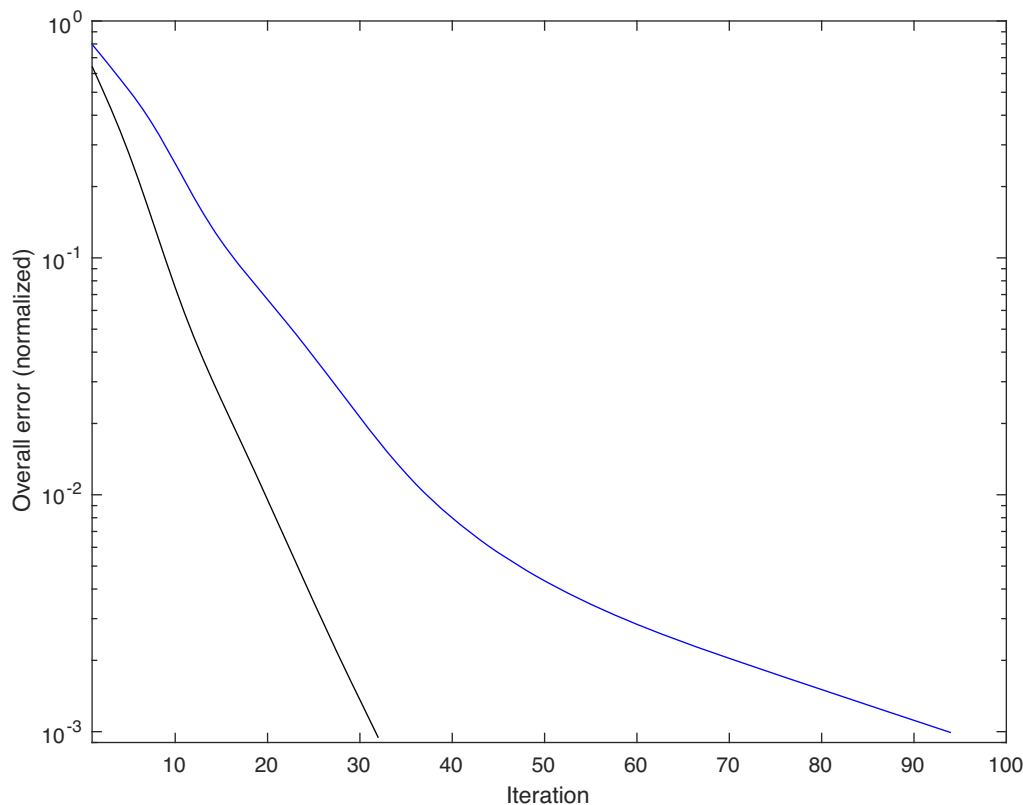
Figure 6. Comparison of overall errors versus the number of iterations for numerical experiments 7–12 described in Table 1.

Figure 7. Comparison of overall errors versus the number of iterations for numerical experiments 6 (optimal HAM series with some dissipation in the reference medium) and 7 (original convergent Born series of Osnabrugge *et al.* 2016). Note that the optimal HAM series (black curve) requires much less iterations than the convergent Born series (blue curve) of Osnabrugge *et al.* (2016).

experiments and found that a scattering series with $\epsilon = 0.5$, $h = -0.8$ and $H = I$ requires much less iterations to converge than the original convergent Born series of Osnabrugge *et al.* (2016). Other choices of the (ϵ, h, H) may lead to even higher convergence rate, but existing guidelines for selecting h and H (see Liao 2003) needs to be modified in the presence of the new parameter ϵ.

Historically, this paper represents a rare example of the application of HAM for solving integral equations and the first example in the context of seismic wavefield modelling. The introduction of the dissipation parameter ϵ into the HAM formalism also represents a novel feature of this work. *Theoretically*, the embedding parameter λ reminds us about the running coupling constant in the renormalization group theory of Jakobsen *et al.* (2019a) as well as the homotopy parameter λ of Watson (1989), but these relations requires further investigation. *Computationally*, it is interesting to note that the computational cost of the reference solution (7) we have obtained via matrix inversion and the scattering series solution (eqs 25–27) scales like N^3 and N^2, respectively, where N is the number of grid blocks in a discretized seismic model. Since our formulation is based on a homogeneous reference medium, it allows for the use of efficient and memory-saving Fast Fourier Transform methods that scales like N and $N \log N$, respectively (see Osnabrugge *et al.* 2016; Jakobsen *et al.* 2019a). The present work can also be combined with convergence acceleration techniques (Eftekhar *et al.* 2018). *Practically*, it is important that the theory and method developed in this study can be generalized to anisotropic elastic media, since the corresponding wave equation can also be transformed into an integral equation of the Lippmann–Schwinger type (Jakobsen *et al.* 2019b). Having developed a convergent forward scattering

series, the next step could be to apply this series in the context of inverse scattering theory. Weglein *et al.* (2003) have pioneered inverse acoustic scattering methods that do not require an assumed propagation velocity model within the medium (Zou & Weglein 2018). Their approach (Zhang & Weglein 2009; Zou *et al.* 2019) is based on the Born series solution of the Lippmann–Schwinger equation and a concomitant expansion of the interaction in orders of the data. In principle, the method is completely general and requires no prior information about the target or the propagation details of the probe signal within the target. The only fundamental limitation of the approach appears to the convergence of the conventional Born series (Kouri & Vijay 2003). Weglein *et al.* (2003) have made significant progress using this approach by introducing subseries. We hope to develop convergent inverse scattering series using the HAM scattering series. However, it is not obvious that the inverse scattering series will converge even though the forward scattering series is convergent. *Finally*, we note that the work reported here may be useful in future applications of the HAM within the context of nonlinear inverse scattering to solve the so-called regularized normal equations (Jegen *et al.* 2001).
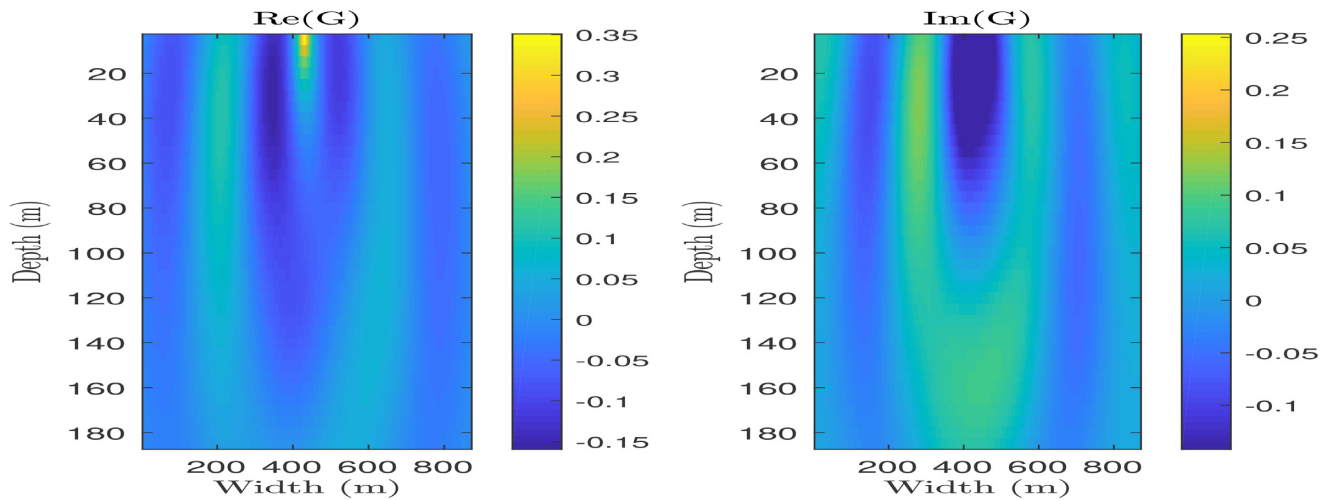
REFERENCES

Abbasbandy, S., 2006. The application of homotopy analysis method to nonlinear equations arising in heat transfer, *Phys. Lett. A.,* **360,** 109–113.

Abubakar, A. & Habashy, T., 2013. Three-dimensional visco-acoustic modeling using a renormalized integral equation iterative solver, *J. Comput. Phys.,* **249,** 1–12.

Carcione, J.M., Herman, G.C. & Kroode, A.P.E., 2002. Seismic modeling, *Geophysics,* **67,** 1304–1325.

Eftekhar, R., Hu, H. & Yingcai Zheng, Y., 2018. Convergence acceleration in scattering series and seismic waveform inversion using nonlinear Shanks transformation, *Geophys. J. Int.,* **214,** 1732–1743.

Eikrem, K.S., Nævdal, G. & Jakobsen, M., 2019. Iterated extended Kalman filter method for time-lapse seismic full-waveform inversion, *Geophys. Prospect.,* **67**(2), 379–394.

Fu, H.S. & Han, B., 2006. A homotopy method for nonlinear inverse methods, *Appl. Math. Comput.,* **183,** 1270–1279.

Haffinger, P.R., 2013. ***Seismic broadband full-waveform inversion by source-receiver refocusing. PhD thesis,*** TUDelft.

Han, B., Fu, H.S. & Li, Z., 2005. A homotopy method for the inversion of a two-dimensional acoustic wave equation, *Inverse Probl. Sci. Eng.,* **13,** 411–431.

Hetmaniok, E., Slota, D., Trawinski, T. & Witula, R., 2014. Usage of the homotopy analysis method for solving the nonlinear and linear integral equations of the second kind, *Math. Modelling Anal.,* **21,** 350–370.

Huang, X. & Greenhalgh, S., 2019. Traveltime approximation for strongly scattering media using the homotopy analysis method, *Geophys. J. Int.,* **66,** 1749–1760.

Huang, X., Jakobsen, M., Naevdal, G. & Eikrem, K.S., 2019a. Target-oriented inversion of time-lapse seismic waveform data, *Commun. Comput. Phys.,* doi:10.4208/cicp.OA-2018-0143 .

Huang, X., Jakobsen, M. & Wu, R.S., 2019b. On the applicability of a renormalized Born series for seismic wavefield modelling in strongly scattering media, *J. Geophys. Eng.,* **17,** 277–299 .

Jakobsen, M., 2012. T-matrix approach to seismic forward modelling in the acoustic approximation, *Stud. Geophys. Geod.,* **56,** 1–20.

Jakobsen, M., Psenik, I., Iversen, E. & Ursin, B., 2019b. Transition operator approach to seismic full waveform inversion in anisotropic elastic media, *Communi. Comput. Phys.,* doi:10.4208/cicp.OA-2018-0197 .

Jakobsen, M. & Ursin, B., 2015. Full waveform inversion in the frequency domain using direct iterative T-matrix methods, *J. Geophys. Eng.,* **12,** 400–418.

Jakobsen, M. & Wu, R.S., 2016. Renormalized scattering series for frequency-domain waveform modelling of strong velocity contrasts, *Geophys. J. Int.,* **206,** 880–899.

Jakobsen, M. & Wu, R.S., 2017. Multi-scale T-matrix completion method in the absence of a good starting model, *Expanded abstract, SEG Annual Meeting.*

Jakobsen, M. & Wu, R.S., 2018. Accelerating the T-matrix approach to full waveform inversion by domain decomposition, *Geophys. Prospect.,* **66,** 1039–1059.

Jakobsen, M., Wu, R.S. & Huang, X., 2019a. Convergent scattering series solutions of the scalar wave equation based on renormalization group theory: application to seismic wavefields modeling, In revision.

Jegen, M.D., Mark, E., Everet, M.E. & Schultz, A., 2001. Using homotopy to invert geophysical data, *Geophysics,* **66,** 1749–1760.

Kirkinis, E., 2008. Renormalization group interpretation of the Born and Rytov approximations, *J. Opt. Soc. Am. A,* **25,** 2499–2508.

Kouri, D.J. & Vijay, A., 2003. Inverse scattering theory: renormalization of the Lippmann-Schwinger equation for acoustic scattering in one dimension, *Phys. Rev. E,* **67,** 046614.

Liao, S., 1998. Homotopy analysis method: a new analytical method for nonlinear problems, *Appl. Math. Mech.,* **19,** 957–962.

Liao, S., 2003. *Beyond Perturbation: Introduction to the Homotopy Analysis Method,* Chapman and Hall.

Liao, S., 2004. On the homotopy analysis method for nonlinear problems, *Appl. Math. Comput.,* **147,** 499–513.

Liao, S., 2009. Notes on the homotopy analysis method: some definitions and theorems, *Commun. Nonlinear Sci. Numer. Simul.,* **14,** 983–997.

Liao, S., 2012. *Homotopy Analysis Method in Nonlinear Differential Equations,* Springer.

Liao, S., 2014. *Advances in the Homotopy Analysis Method,* World Scientific Publishing.

Malovichko, M., Khokhlova, N., Yavicha, N. & Zhanov, M., 2018. Acoustic 3D modeling by the method of integral equations, *Comput. Geosci.,* **111,** 223–234.

Morse, P.M. & Feshback, H., 1953. *Methods of theoretical physics,* McGraw-Hill Science/Engineering/Math.

Newton, R.G., 2002. *Scattering theory of waves and particles,* Dover Publications.

Oristaglio, M.L. & Blok, H., 2012. *Wavefield Imaging and Inversion in Electromagnetics and Acoustics,* Cambridge Univ. Press.

Osnabrugge, G., Leedumrongwatthanakun, S. & Vellekoop, I.M., 2016. A convergent Born series for solving the inhomogeneous Helmholtz equation in arbitrarily large media, *J. Comput. Phys.,* **322,** 113–124.

Palit, A. & Datta, D.P., 2016. Comparative study of homotopy analysis and renormalization group methods on Rayleigh and Van der Pol equations, *Differ. Equ. Dyn. Syst.,* **24,** 417–443.

Pfeffer, T., 2019. Homotopy and renormalization group approaches for strongly correlated systems, *Doctoral dissertation*, LMU.

Pike, R. & Sabatier, P., 2000. *Scattering: Scattering and Inverse Scattering in Pure and Applied Science,* Academic press.

Robertsson, J.O.A., Blanch, J.O., Nihei, K. & Tromp, J., 2012. *Numerical Modeling of Seismic Wave Propagation: Gridden Two-Way Wave Equation Methods,* Society of Exploration Geophysicists.

Watson, L.T., 1989. Globally convergent homotopy methods: a tutorial, *Appl. Math. Comput.,* **31,** 369–396.

Weglein, A. B., Araújo, F.V., Carvalho, P.M., Stolt, R.H., Matson, K.H., Coates, R.T. & Zhang, H., 2003. Inverse scattering series and seismic exploration, *Inverse Probl.,* **19**(6), R27.

Weinberg, S., 1963. Quasi-particles and the Born series, *Phys. Rev.,* **131**(1), 440–460.

Zhang, H. & Weglein, A.B., 2009. Direct nonlinear inversion of 1D acoustic media using inverse scattering subseries, *Geophysics,* **74**(6), WCD29–WCD39.

Zou, Y., Ma, C. & Weglein, A.B., 2019. A new multidimensional method that eliminates internal multiples that interfere with primaries, without damaging the primary, without knowledge of subsurface properties, for off-shore and on-shore conventional and unconventional plays, in *SEG Technical Program Expanded Abstracts 2019,* pp. 4525–4529.

Zou, Y. & Weglein, A.B., 2018. ISS Q compensation without knowing, estimating or determining Q and without using or needing low and zero frequency data, *J. Seism. Explor.,* **27,** 593–608.

APPENDIX A: DESCRIPTION AND IMPLEMENTATION OF THE HAM SERIES

Similar to the conventional Born series, every iteration is associated with multiple scattering processes of different orders. However, we have reorganized the different terms in the conventional Born series so that the spectral radius of M is smaller than unity. This implies that each new term is smaller than the previous one, so that the scattering series does not diverge when the number of iterations becomes large. Mathematically, this is done by introducing an integral operator with spectral radius smaller than unity via the use of control parameter h and the convergence control operator H. The series converges if the spectral radius of the operator M is less than unity. We have also introduced an element of dissipation in the reference medium, which ensures that the energy associated with Greens function is finite and localized. It should be emphasized that the dissipation parameter ϵ can be selected arbitrarly. This is because the dissipation is compensated exactly by a corresponding gain term in the scattering potential, suggesting that the final results
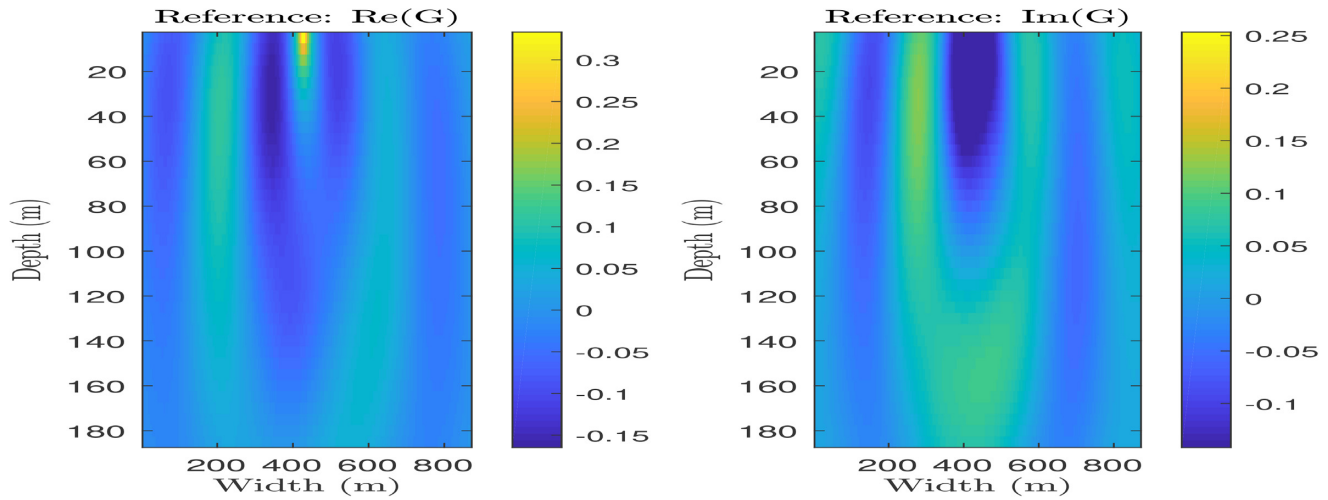
Figure A1. The real and imaginary parts of the frequency-domain wavefield at 10 Hz computed by solving the Lippmann–Schwinger equation exactly using a real space matrix representation.

Figure A2. The real and imaginary parts of the frequency-domain wavefield computed using the HAM series with auxiliary parameters corresponding with experiment 11 in Table 1.

are independent of this dissipation in the reference medium. The dissipation aspect of our HAM algorithm is similar to the convergent Born series of Osnabrugge *et al.* (2016). However, our convergent scattering series is more general than the convergent Born series, since the convergent control parameters can be selected rather arbitrary, as long as the spectral radius of the M-operator is smaller than unity. Some details for implementation of the new convergent scattering series using based on the HAM are provided in Algorithm 1. In addition, Table 1 shows the norm $\|M\|$ and spectral radius $\sigma(M)$ of the operator M with numerical experiments.

The HAM algorithm is represented by eqs (25)–(27). However, the formulation in the main text is based on the real-space coordinate representation of the relevant integral operators. As discussed by Osnabrugge *et al.* (2016), the operation of Green's function with contrast-source terms has a convolution structure that can be implemented more efficiently by using the wave vector representation; that is, by using the fast Fourier transform (FFT) algorithm in this

context. This is because convolution in real-space is equivalent to multiplication in the Fourier space, and the computational cost of the FFT-operation is much smaller than that of matrix multiplication and inversion. The memory requirements scale like N^2 and N when using the position and wave vector representations, respectively. The computational cost should theoretically scale like N^3 and $N \log N$ when using the position and wave vector representations, respectively. The iterative FFT algorithm is implemented as

$$\psi_m(\mathbf{r}) = hH(\psi^{(0)}(\mathbf{r}) - \psi_0(\mathbf{r}) \\ - \text{ifft}\left[G^{(0)}(\mathbf{k}) \, \text{fft}\left[V\psi_m(\mathbf{r})\right]\right]), \tag{A1}$$

where fft and ifft are the forward and inverse fast Fourier transform operators, $\mathbf{k}$ is the Fourier transformed coordinates. Figs A1 and A2 show the frequency-domain wavefield using exact solutions, the efficient and memory-saving FFT implementation with 100 iterations, respectively.

Algorithm 1 Pseudo code for the scattering series

Initialisation: frequency, maximum iteration number N_{max}, the parameter ϵ

true model and background model;

$V = k^2 - k_0^2 - i\epsilon$

$k_b = \sqrt{k_0^2 + i\epsilon}$

$\psi^{(0)} = G^{(0)}S$

$\psi = \psi^{(0)}$

$M = I + hH - hHG^{(0)}V$

$n = 1$

while $n < N_{max}$ **do**

  $n = n + 1$

  if $n == 1$ **then**

    $\psi_m = hH(\psi^{(0)} - \psi_0 - G^{(0)}V\psi^{(0)})$

  else

    $\psi_m = M\psi_m$

  end if

  $\psi = \psi + \psi_m$

end while